Available online at www.sciencedirect.com

ScienceDirect

Procedia Engineering 207 (2017) 1445–1450

Procedia Engineering

www.elsevier.com/locate/procedia

International Conference on the Technology of Plasticity, ICTP 2017, 17-22 September 2017, Cambridge, United Kingdom

Modelling of High Pressure Torsion using FEM

Roman Kulagin[a,]*, Yan Beygelzimer[b], Yulia Ivanisenko[a], Andrej Mazilkin[a,c], Horst Hahn[a]

[a]*Institute of Nanotechnology (INT), Karlsruhe Institute of Technology (KIT), Hermann-von-Helmholtz-Platz 1, 640, 76344 Eggenstein-Leopoldshafen, Germany*

[b]*Donetsk Institute for Physics and Engineering named after O.O. Galkin, NASU, Vernadsky Str. 46, 03142 Kyiv, Ukraine*

[c]*Institute of Solid State Physics, RAS, Academician Ossipyan Str.2, 142432 Chernogolovka, Russia*

Abstract

High Pressure Torsion (HPT) is historically the first and is currently most common process of the severe plastic deformation (SPD). HPT is used for producing nanocrystalline structures in metals and alloys, as well as for cold welding of powders. The result of the HPT treatment is determined by the flow kinematics and the stress state of a material under deformation. P. Bridgman proposed a simple model for the initial assessment of shear strain in the sample during HPT. A number of recent investigations show that the true plastic flow during HPT can differ significantly from the simple model. We present in our report results of the FEM investigation of different types of flow during HPT. We propose a hypothesis that the vortex formation during the SPD process is caused by the local blocking of simple shear in a material under deformation.

Peer-review under responsibility of the scientific committee of the International Conference on the Technology of Plasticity.

Keywords: severe plastic deformation, high pressure torsion, FEM, vortex

1. Introduction

High Pressure Torsion (HPT) is a widely used process for modifying the materials´ structure and properties by means of severe plastic deformation [1]. It is a generally accepted assumption that deformation during HPT takes

* Corresponding author. Tel.: +49 (721) 608-28127
E-mail address: roman.kulagin@kit.edu

1877-7058
Peer-review under responsibility of the scientific committee of the International Conference on the Technology of Plasticity.
10.1016/j.proeng.2017.10.911

place through a simple shear. The shear is uniform over the sample's thickness and shear strain in each point of the sample is directly proportional to the distance r from the axis of anvils rotation:

$$\gamma \sim \beta \times r \tag{1}$$

Experiments and numerical simulations in recent years show that the actual plastic flow during HPT may differ significantly from this simple scheme. For example, calculations by finite element modeling (FEM) show the inhomogeneity of the stress-strain state over the sample thickness [2]. In [3] dead metal zones were found at the edge of the sample. Double-swirl flow pattern in a plane perpendicular to the rotation axis was experimentally recorded in [4]. Recent studies show that vortices in the sample´s tangential direction may occur in the layered materials after the HPT processing [5]. These results indicate that the plastic flow during HPT may be of a rather complex nature, which must be considered when applying the process.

In the present study, we identified possible modes of HPT and defined conditions when they are realized. It is shown that depending on mechanical properties and structure of a material, deformation during HPT may occur in both laminar and turbulent flows of different space-time modes.

2. Laminar flow of the material during HPT

The set-up for the HPT process is shown in Fig. 1.

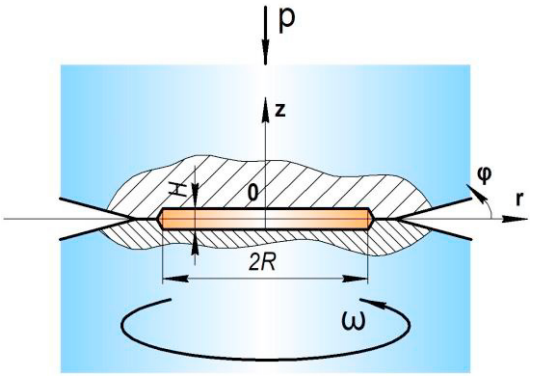

Fig. 1. Schematic geometry of HPT.

In this section, we examine the laminar flow of the material during HPT, which is characterized by the following velocity field: $v_r=0, v_z=0, v_\varphi= v_\varphi(r,z,\beta)$, where r, z, φ are the cylindrical coordinates (see Fig. 1) and β is the angle of the anvils rotation. First, we consider the conditions under which stationary flow takes place, i.e. it does not depend on β. In other words, we determine the conditions when β is not included in the equation for plastic flow. For stationary flow $v_r=0, v_z=0, v_\varphi= v_\varphi(r,z)$. It follows from last expressions that von Mises strain rate $\dot{e}_M = \dot{e}_M(r,z)$ and the von Mises strain is

$$e_M = \int_0^t \dot{e}_M dt = \int_0^\beta \dot{e}_M \frac{d\beta}{\omega} = \frac{\beta}{\omega}\dot{e}_M(r,z) \tag{2}$$

in this case, where t is the time and ω is the angular velocity of the anvils rotation.

It follows from the associative law for the plastic flow that

$$\frac{\dot{e}_{ij}}{\dot{e}_M} \sim \frac{\sigma_{ij} - \sigma\delta_{ij}}{\bar{\sigma}} \tag{3}$$

where σ is the hydrostatic stress, and $\bar{\sigma}$ is the equivalent stress.

According to Eq. (3), the stress tensor components can be calculated as a product of two separate functions, i.e.,

$$\sigma_{ij}(\beta, r, z) = \Phi(\beta)\sigma_{ij}^*(r, z) \tag{4}$$

where $\Phi(\beta)$ and $\sigma_{ij}^*(r,z)$ are functions of β and (r,z) respectively.

If Eq. (4) is not true, then the left part of Eq. (3) depends on β, and the right part does not depend, which is not possible. From the Eq. (4) one can get:

$$\bar{\sigma} = \Phi(\beta)\bar{\sigma}^*(r, z) \tag{5}$$

The von Mises plasticity condition is:

$$\bar{\sigma} = \sigma_S \tag{6}$$

where $\sigma_S(e_M, \dot{e}_M)$ is the flow stress of the deforming material.

Taking into account Eqs. (2) and (5), we obtain the following expression:

$$\Phi(\beta)\bar{\sigma}^*(r, z) = \sigma_S\left(\frac{\beta}{\omega}\dot{e}_M, \dot{e}_M\right) \tag{7}$$

Rotation angle β is excluded in this expression if the function $\sigma_S(e_M, \dot{e}_M)$ is homogeneous by its first term, i.e.

$$\sigma_S(e_M, \dot{e}_M) = e_M^n f(\dot{e}_M) \tag{8}$$

where $f(\dot{e}_M)$ is a function of the strain rate. In this case we obtain from the Eq. (8):

$$\Phi(\beta)\bar{\sigma}^*(r, z) = \left(\frac{\beta}{\omega}\right)^n \dot{e}_M^n f(\dot{e}_M) \tag{9}$$

and when $\Phi(\beta) \sim \beta^n$, then we can reduce β in both parts of the relation.

Based on the analysis, we conclude that power strain hardening law is a necessary condition for stationary plastic flow during HPT. It is shown that this condition is also sufficient for the stationary state of HPT [6].

It was shown in [7] that the power law strain hardening is associated with the development of a self-similar microstructure in materials during plastic deformation and corresponds to experimental observations in a certain range of von Mises strains. As the deformation exceeds this range, then both the microstructure and the strain hardening of the material reach a saturation level, and the power law is no longer valid. The saturation of work hardening during HPT should lead to the strain localization in a thin layer of the sample in case the strain rate hardening is absent [7]. We will show by means of FEM numerical simulations that the strain rate hardening may in this case stabilize the plastic flow during HPT and prevent strain localization.

All calculations were done in the DEFORM – 2D/3D software using a 2D axisymmetric torsion model [8]. Two stress–strain curves from [6] obtained from experimental stress–strain curve of the Fe powder processed by HPT [9] were used for our calculations. The curves were modified to take into account the strain rate hardening:

$$\sigma_s[MPa] = 740 e_M^{0.18} \left(\frac{\dot{e}_M}{a} \right)^b \tag{10}$$

$$\sigma_s[MPa] = [1050 - 463 \cdot exp(-0.39 e_M)] \cdot \left(\frac{\dot{e}_M}{a} \right)^b \tag{11}$$

where a and b are the parameters of the strain rate hardening.

The first term in Eq. (11) is an approximation of the experimental stress–strain curve of the Fe powder obtained in [9] under the condition of HPT. The first term in the Eq. (10) is the power law, which approximates this curve for the strain values $1 < e_M < 5$.

To illustrate the effect of stain rate hardening on the plastic flow at HPT, we have carried out five numerical experiments. Conditions of the experiments are summarized in Table 1. In all experiments $a = 0.05 s^{-1}$, the sample diameter was 10 mm, and its thickness was 1 mm. The strain rate value in (10) and (11) was normalized in accordance with the average strain rate value for the HPT conditions in [6].

Table 1. Parameters for the stress–strain curves in FEM simulations.

Experiment	1	2	3	4	5
Strain-Stress curve	Eq. 10	Eq. 11	Eq. 11	Eq. 11	Eq. 11
Parameter b	-	0	0.005	0.05	0.5

Results of the numerical calculations are shown in Fig. 2.

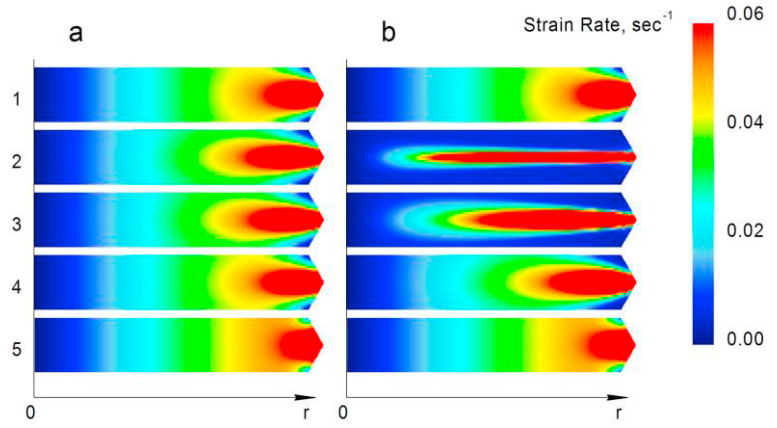

Fig. 2. Maps of the von Mises strain rate in the (r, z) plane (FEM simulation) at the anvils rotation angle $\beta = 0.5\pi$ (a) and $\beta = 3.5\pi$ (b); the numbering in figure corresponds to the Table 1.

As it can be seen in Fig. 2a, for small rotation angles β, i.e. before the work hardening reaches the saturation level, the power-law in Eq. (10) is valid, the sample is deformed practically according to Eq. (1). For larger values of β and small values of strain rate sensitivity b, deformation is localized around the geometrical shear plane (Fig. 2b, cases 2, 3). But when the strain rate sensitivity of the material is large enough (similar to superplastic flow i.e. > 0.3, Fig. 2b case 5), the sample is deformed according to Eq. (1). The intermediate case when $b = 0.05$ (Fig. 2b, case 4) is rather interesting because the strain localization is not very pronounced and shear strain is distributed almost according to Eq. (1). Ultrafine-grained materials processed by HPT usually have strain rate sensitivity coefficient in the range $0.01 \div 0.1$ [10, 11], which shows that Eq. (1) still can be applied as a rough estimate for the shear strain at HPT.

3. Turbulent flow of the material during HPT

Recent studies on a layered material subjected to the HPT deformation revealed the formation of vortices forming perpendicular to the radial direction of samples [5]. The vortices looked very similar to those observed during the turbulent flow of liquids or gases. This kind of behavior was observed earlier in other processes of plastic shear, such as the friction test [12] or the scratch test with a diamond indenter [13].

In [5, 12, 13] the formation of vortices during the plastic shear was associated with the development of Kelvin-Helmholtz instability [14]. This instability appears at the interface between two fluids moving relative to each other. We propose a different explanation to this phenomenon.

From the physical point of view, the Kelvin-Helmholtz instability is associated with the pressure increase in a moving medium in the location of the expansion of its flow. This pressure difference leads to the stability loss at the interface between two liquids followed by the formation of vortices [14]. For the instability to form, the stresses in the medium due to inertial forces must be of the same order of magnitude as the stresses caused by internal forces. Inertial stresses are proportional to ρv^2 [14], where ρ and v are the density and flow velocity of the medium, respectively.

The magnitude of the internal stresses in a plastically deformed solid body is of the order of its yield stress *YS*. In this case, the ratio of inertial stress to the internal stress can be assessed as $\kappa=\rho v^2/YS$. For instance, for copper $\rho=8900kg/m^3$, $YS=300MPa$; and for the flow rates which are typical during HPT $v=1mm/sec$, we obtain $\kappa\sim10^{-11}$, i.e. the inertial stresses during the HPT process can be neglected. This means that the physical mechanism leading to the Kelvin-Helmholtz instability in liquids is not valid for slow deforming metals. Despite the similarity of the appearance, random vortices in solids and liquids have different physical nature.

In [15] the formation of vortices in a material plastically deformed through simple shear is associated with the local blocking of the shear deformation. Based on FEM numerical modeling, it will be shown that the local blocking of shear in the sample leads to twists and turns of the obstacles. We regard it as the physical reason for the turbulent flow during shear straining.

Layer 1 of plastic material is located between two dies, moving in opposite directions; see Fig. 3a and Fig. 3b. The distance between the dies does not change, and friction forces between the dies and the material are sufficient to prevent any slippage. In the layer 1, there is an obstacle 2, locally blocking shear. The obstacle has the shape of a cylinder with its axis oriented perpendicular to the plane of the figure (Fig. 3a) or of a thin lamella (Fig. 3b). We assume that the yield stress of the obstacle is ten times higher than that of the material in the layer 1.

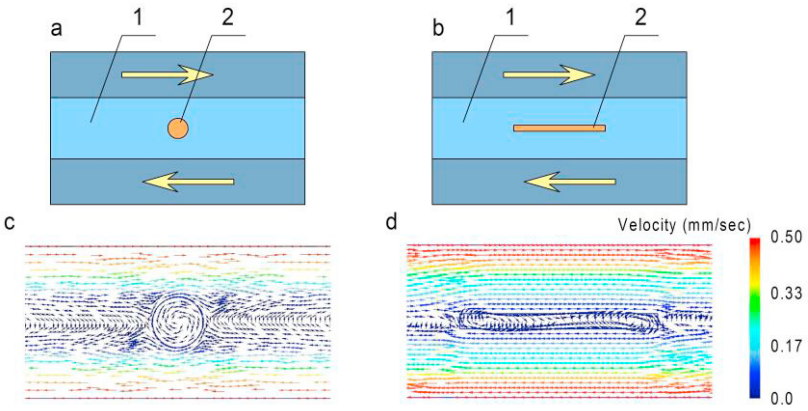

Fig.3 Simple shear blocked locally by an obstacle: a, b – schemes for the simulations; c, d – velocity fields.

The results of the FEM model (see Fig. 3c and Fig. 3d) indicate that the local blocking of shear indeed causes twists and turns of the obstacles, which leads to the formation of vortices at sufficiently large shear strain. Different types of the material non-uniformity can serve as obstacle during the HPT deformation. In particular, in the case of

layered materials, the layers with higher strength and hardness can serve as such obstacles. These shear lock points gradually transform into a chain of vortices as a result of the twists and turns of the obstacles.

Practical application of these effects is possible for the production of bulk composite billets with a vortex architecture by the High Pressure Torsion Extrusion process [16].

4. Summary

Based on the presented above analysis, the following conclusions can be made:

- Depending on the structure and properties of the material under the deformation, the plastic flow during HPT may be either laminar or turbulent. Stationary laminar plastic flow requires the power law function of work hardening.
- If the strain rate hardening is absent and the work hardening levels off, then the deformation will be localized in the thin layer of the sample close to the geometrical shear plane. When the strain rate sensitivity coefficient of the material is high enough, then strain localization will not take place.
- The physical reason for turbulence is a local blocking of simple shear in some areas of the sample. The latter may be due the presence of inclusions in a material with higher strength and hardness.

It should also be noted that these conclusions are based on the results of numerical simulation. Further investigations on experimental validation of these effects are the subject of our future work.

Acknowledgements

YB would like to express his gratitude to the State Fund for Fundamental Research of the Ukraine for financial support of research on vortex flow under severe plastic deformation through the competitive grant F71/56-2016.

RK and YI acknowledge funding support from the German Research Foundation (DFG) under Grant IV98/8-1.

References

[1] A.P. Zhilyaev, T.G. Langdon, Using high-pressure torsion for metal processing: Fundamentals and applications, Prog. Mater Sci. 53 (2008) 893–979.

[2] R.B. Figueiredo, M.T.P. Aguilar, P.R. Cetlin, T.G. Langdon, Analysis of plastic flow during high-pressure torsion, J. Mater. Sci. 47 (2012) 7807–7814.

[3] D.J. Lee, E.Y. Yoon, L.J. Park, H.S. Kim, The dead metal zone in high-pressure torsion, Scripta Mater. 67 (2012) 384–387.

[4] Y. Cao, M. Kawasaki, Y.B. Wang, S.N. Alhajeri, X.Z. Liao, W.L. Zheng, S.P. Ringer, Y.T. Zhu, T.G. Langdon, Unusual macroscopic shearing patterns observed in metals processed by high-pressure torsion, Mater. Sci. 45 (2010) 4545–4553.

[5] M. Pouryazdan Panah, Shear-Induced Mixing in Metallic Systems, PhD Thesis, Darmstadt, Germany, 2015

[6] Y. Beygelzimer, R. Kulagin, L.S. Toth,Y. Ivanisenko, The self-similarity theory of high pressure torsion, Beilstein J. Nanotechnol. 7 (2016) 1267–1277.

[7] Y. Beygelzimer, L.S. Toth, J.J. Jonas, Some Physical Characteristics of Strain Hardening in Severe Plastic Deformation, Adv. Eng. Mater, 17 (2015) 1783–1791.

[8] DEFORM v11.0 Documentation, Scientific Forming Technologies Corporation, http://www.deform.com/

[9] Y.J. Zhao, R. Massion, T. Grosdidier, L.S. Toth, Gradient Structure in High Pressure Torsion Compacted Iron Powder, Adv. Eng. Mater. 17 (2015) 1748–1753.

[10] N. Chinh, P. Szommer, Z. Horita, T. Langdon, Mater Sci Forum (2006) 503–504:1001;

[11] R. Valiev, M. Murashkin, A. Kilmametov, B. Straumal, N. Chinh, T. Langdon, J Mater Sci, 45 (2010) 4718–4724.

[12] H.-J. Kim, S. Karthikeyan, D. Rigney, A simulation study of the mixing, atomic flow and velocity profiles of crystalline materials during sliding. Wear 267 (2009) 1130–1136.

[13] Narayan K. Sundaram, Yang Guo, and Srinivasan Chandrasekar Mesoscale Folding, Instability, and Disruption of Laminar Flow in Metal Surfaces. PRL 109 (2012) 106001.

[14] L. Prandtl, O.G. Tietjens, Fundamentals of Hydro - and Aeromechanics, Dover Pub. Inc., New York, 1957.

[15] Y. Beygelzimer, Vortices and Mixing in Metals during Severe Plastic Deformation, Mater. Sci. Forum 683 (2011) 213–224.

[16] Y. Ivanisenko, R. Kulagin, V. Fedorov, A. Mazilkin, T. Scherer, B. Baretzky, H. Hahn, High Pressure Torsion Extrusion as a new severe plastic deformation process, Mater. Sci. Eng., A, 664 (2016) 247–256.